

## Ni-P TiO<sub>2</sub> Nanoparticle Composite Formed by Chemical Plating: Deposition Rate and Corrosion Resistance

Li Yongfeng<sup>1,\*</sup>, Zhao Limin<sup>2</sup>, Wang Zhankui<sup>1</sup>, Ma Lijie<sup>1</sup>, Su Jianxiu<sup>1</sup>, Liu Chang<sup>1</sup>, Jiao MingChao<sup>1</sup>

<sup>1</sup> School of Mechanical and Electrical Engineering, Henan Institute of Science and Technology, Xinxiang, 453003, China

<sup>2</sup> Management Institute, Xinxiang Medical University, Xinxiang 453003, China

\*E-mail: [yongfengli121@outlook.com](mailto:yongfengli121@outlook.com)

Received: 24 October 2016 / Accepted: 12 February 2017 / Published: 12 March 2017

---

We studied the parameters influencing the chemical plating deposition rate of Ni-P TiO<sub>2</sub> nanoparticle composite layers and the corrosion resistance of the resulting layers. The amount of TiO<sub>2</sub> added, plating time, temperature and pH values were factors in a four-factor three-level orthogonal test; the parameters influencing the deposition rate of the Ni-P TiO<sub>2</sub> nanoparticle composite plating layer were optimized. A specimen featuring the composite plating layer was prepared under the optimized conditions and its corrosion resistance was compared with those of a Ni-P plating layer and a carbon steel matrix. Our results indicated that the corrosion resistance of the Ni-P TiO<sub>2</sub> nanoparticle composite plating layer was better than that of the Ni-P plating layer in the 3.5% NaCl solution, and the corrosion resistance of the Ni-P plating layer was slightly higher than that of the Ni-P TiO<sub>2</sub> nanoparticle composite plating layer which immersed in the 10% H<sub>2</sub>SO<sub>4</sub> and 15% HCl solution. Furthermore, both these layers showed better corrosion resistances than that of the carbon steel matrix. The corrosion resistance mechanism of the nanometer composite plating layer was discussed.

---

**Keywords:** chemical plating, composite nanomaterial, deposition rate, corrosion resistance

### 1. INTRODUCTION

Chemical plating is a process where metal ions in a plating solution are reduced on the surface of a specimen to be plated, forming a metal layer. Chemical plating is performed under catalytic reducing conditions without the application of an external potential[1]. The technology has the advantages of simple equipment requirements and the ability to apply a plating layer with an even thickness and with no clear edge effect[2]. Thus, chemical plating is particularly applicable to coating the surfaces of complex shapes. Furthermore, chemical plating can coat the interior surfaces of pipelines, valves and other components, and is suitable for use with various materials, including

metals, plastics, glasses, and ceramics. Chemically plated layers often have high hardness, excellent abrasion and corrosion resistance and are widely applied to protect surfaces in a variety of fields such as aviation, electronics, petroleum extraction, and automobile manufacture[2, 3].

The pH value of the plating solution used during nickel phosphorous chemical plating is an important parameter that influences the structure of the resulting nickel plating. At low pH values, the plating speed decreases, the phosphor content in the plating layer increases, and Ni-P alloys form with amorphous structure when the P content is higher than 6%. Phosphate solubility increases at low pH, which makes the plating layer smooth and clear. Furthermore, increasing temperature improves ion diffusion and the reactivity. Temperature is another important parameter, which influences the deposition rate of chemical plating layers.

Unfortunately the properties of pure chemical plated Ni-P alloys require further improvements to enable more widespread application[4-6]. New developments in nanotechnology may allow further improvements to be made through the use of composite plating layers. Nanoscale materials have unique properties owing to their small particle sizes, such as high surface areas and quantum confinement effects. Solid nanometer-sized particles may improve dispersion effects in composite plating of matrix surfaces[2, 7, 8]. When insoluble nanoparticles are dispersed in a chemical plating solution, particles that deposit on the matrix metal surface can improve the performance of the resulting composite plating layer[9, 10]. Composite plating layers with embedded nanoparticles may feature improved hardness, and greater resistance to abrasion, corrosion, and high-temperature oxidization resistance[11, 12]. Currently, the research of the nanocomposite Ni-P plating is mainly to add nanoparticle such as SiC[13, 14], TiO<sub>2</sub>[15-17], ZrO<sub>2</sub>[18], SiO<sub>2</sub>[19], PCTFE[20], MoS<sub>2</sub>[21], Al<sub>2</sub>O<sub>3</sub>[8, 22] and etc.

The aim of this study is to optimize the parameters for forming Ni-P layers embedded with TiO<sub>2</sub> nanoparticles through a four-factor three-level orthogonal test. We studied factors including the amount of TiO<sub>2</sub> nanoparticles added, plating time, temperature, and the plating solution pH value. We compared the corrosion resistances of the resulting Ni-P alloys, Ni-P TiO<sub>2</sub> nanoparticle composite layers, and matrix carbon steel. The corrosion resistance properties of these layers were related to their morphologies and composition.

## 2. EXPERIMENT AND METHODS

### 2.1 Sample Preparation

The specimen matrix used in the test was Q235 cold-rolled steel sheet with a size of 40 mm×25 mm×1.5 mm. The surface of the plating specimen was pretreated before chemical plating. The pretreatment was as follows: initially oil on the specimen was removed with detergent; the specimen was cleaned with distilled water; residual oil on the specimen was removed with a chemical alkali solution; the specimen was cleaned with distilled water; dust was removed from the specimen with 15% HCL (10 to 20 min); the specimen was cleaned with distilled; the specimen was activated with 5% HCL (10 to 20S); the specimen was cleaned with distilled water.

**Table 1.** Components of alkali cleaning solution and technological condition

Composition	Concentration	Component	Concentration
NaOH(g/L)	20 ~ 40	Na <sub>2</sub> SiO <sub>3</sub> (g/L)	5 ~ 15
Na <sub>2</sub> CO <sub>3</sub> (g/L)	20 ~ 30	OP-10 emulsifier (g/L)	1 ~ 3
Na <sub>3</sub> PO <sub>4</sub> ·12H <sub>2</sub> O(g/L)	5 ~ 10		

Temperature 80–90 °C.

## 2.2 Preparation of the composite plating solution

The formula of the Ni-P chemical plating basic plating solution used in the test was as follows: NiSO<sub>4</sub>·6H<sub>2</sub>O, 30 g/L; lactic acid, volume percentage 3%; citric acid, 25 g/L; sodium acetate, 20 g/L; NaH<sub>2</sub>PO<sub>2</sub>·H<sub>2</sub>O, 25 g/L; pH = 4.4, and the temperature was 80°C. Ensuring that the TiO<sub>2</sub> nanoparticles were well dispersed in the composite plated layer was an essential part of our experiments. Chemical and physical dispersion methods were used to ensure sufficient dispersion of the TiO<sub>2</sub> nanoparticles in the plating solution. The chemical dispersion was performed as follows: an anion surfactant, lauryl sodium sulfate, was added to the plating solution, before addition of the nanoparticles. The physical dispersion methods included ultrasonication and mechanical stirring. After the TiO<sub>2</sub> nanoparticles were added to the plating solution, the mixture was ultrasonicated with a Q-100DE ultrasonicator at 20 W and 20 kHz for 10 min. Then the plating solution was mechanically stirred with a magnetic stirrer. The main components of the composite plating solution were as follows:

**Table 2.** Components of composite plating solution

Component	Concentration	Component	Concentration
Nickel sulfate	30g/L	A	2.5mg/L
Lactic acid	Volume percentage 3%	Lauryl sodium sulfate	40mg/L
Citric acid	25g/L	Sodium monophosphate	25g/L
Sodium acetate	20g/L		

After the pretreatment the specimens were placed into the plating solutions for composite plating over a certain time. After plating the specimens were removed from the solution, cleaned with cold distilled water, and dried for the performance testing. The plating temperature was measured with an electronic thermometer, and pH was measured with an electronic pH meter. In addition, an H.H.S 21-40 constant-temperature water bath was used to maintain the solution temperature during the plating process, and a rotary device was used to ensure even plating of the test specimen. An air pump was used to agitate and mix the plating solution.

### 2.3 The orthogonal test

In order to optimize the plating parameters for the Ni-P TiO<sub>2</sub> nanoparticle composite layers under acidic conditions, we studied the amount of TiO<sub>2</sub> nanoparticles added, plating time, temperature and solution pH as factors in a four-factor three-level orthogonal test. The amount of TiO<sub>2</sub> nanoparticles added is 2g/L, 3g/L and 4g/L, respectively. The plating time is 0.5 h, 1 h and 1.5 h. The temperature is 75 °C, 80 °C and 85 °C. The pH value is 4, 5 and 6. The variables that were assessed included the deposition speed of the plating layer and the rate of corrosion of the plating layer in standard corrosion solutions.

### 2.4 Performance of nanometer composite plating layer

#### 2.4.1 Micro-morphology and structural analysis of the plating layer

We observed the morphology of the plating layer with a Quanta 200 scanning electron microscope and the elemental composition of the plating layer was measured by energy dispersive spectrometry.

#### 2.4.2 Measurement of deposition rate of composite plating solution

Typically, deposition rate can be measured from the change in the layer thickness and by measuring the change in specimen weight. Here, we used the weighing method: formula (1) was used to determine the plating speed.

$$v = (W_2 - W_1) / (s \cdot \rho \cdot t) \times 10^4 \quad (1)$$

Where:

$v$  is the deposition rate of the plating layer ( $\mu\text{m/h}$ );

$W_1$  is the mass before the test block was plated (g);

$W_2$  is the mass of the test block after plating (g);

$\rho$  is the density of alloy plating layer ( $\text{g/cm}^3$ );

$s$  is the plating surface area of the test block ( $\text{dm}^2$ );

$t$  is the plating time (h)

#### 2.4.3 Corrosion resistance

##### 1) Polarization curves to determine self-corrosion potential of the plating layer

An AUTOlabs electrochemical work station was used to measure the polarization curves of the specimen layers at room temperature in a corrosive medium: 3.5% NaCl solution. We used a scanning speed of  $-0.1 \text{ mV.s}^{-1}$ , a potential interval of 0.5 mV, an initial potential of  $-0.6 \text{ V}$ , and a termination potential of  $-0.1 \text{ V}$  with a saturated calomel reference electrode and a platinum auxiliary electrode.

The polarization curves of all the plating layers were tested and the self-corrosion potentials of the plating layers were obtained.

## 2) Immersion corrosion test

The plating layer was immersed in standard corrosive solutions of 10% H<sub>2</sub>SO<sub>4</sub> and 15% HCl at the room temperature for 9 h. The specimens were then removed from the solutions, cleaned, dried and weighed. The mass difference of the test specimens before and after the corrosion test was used as a measure of the corrosion resistance.

# 3. RESULTS AND DISCUSSION

## 3.1 Optimization of parameters for Ni-P TiO<sub>2</sub> nanoparticle composite plating

Table 3 shows the conditions used in the L9 (3<sup>4</sup>) orthogonal test.

**Table 3.** L9 (3<sup>4</sup>) orthogonal test

Factor	TiO <sub>2</sub> (g/L)	Time (h)	Temperature (°C)	pH	Deposition rate (μm/h)	Corrosion amount (g)
Test 1	2	0.5	80	4	11.25	0.0401
Test 2	2	1	75	5	7.82	0.0257
Test 3	2	1.5	85	6	13.07	0.0377
Test 4	3	0.5	75	6	9.66	0.0388
Test 5	3	1	85	4	12.4	0.0358
Test 6	3	1.5	80	5	10.53	0.0233
Test 7	4	0.5	85	5	15.15	0.0288
Test 8	4	1	80	6	12.61	0.0243
Test 9	4	1.5	75	4	6.28	0.0422

Previous studies on the preparation and corrosion resistance of Ni-P TiO<sub>2</sub> composite plating nanoparticle have been carried out by different methods and parameters[16, 23-25]. In the present work, the effects of process parameters on deposition rate and corrosion rate are investigated from four aspects: TiO<sub>2</sub> addition, plating time, solution temperature and pH value.

## 3.2 Influence of the amount TiO<sub>2</sub> nanoparticles added on the deposition rate of the composite plating layer

Single factor analyses were performed on the orthogonal test results. The influence of the amount of TiO<sub>2</sub> nanoparticles added to the plating solution on the deposition rate of the composite plating layer is illustrated in Table 3. The plating speed increased as the amount of TiO<sub>2</sub> nanoparticles was increased. The maximum plating speed was achieved when 3 g/L of TiO<sub>2</sub> nanoparticles were added to the solution. Further increases in the amount of TiO<sub>2</sub> nanoparticles caused a decrease in the

plating speed. The initial increase in deposition rate as the amount of  $\text{TiO}_2$  nanoparticles was increased can be explained by the flushing and abrasion action of  $\text{TiO}_2$  in the plating solution under the stirring action. This effect increased the number of active surface sites on the plating specimen, and reduced the speed of metal particles, increasing the deposition rate. However, for large amounts of nanoparticles, the probability of the particles attaching to the plating specimen surface increased. This may reduce the number of active sites on the plating specimen surface, which adversely affected the deposition rate of the plating layer. With all other conditions stable, the most rapid plating layer deposition rate was at a  $\text{TiO}_2$  nanoparticle content of 3 g/L. Komal Yadav et al.[25] have found that the concentration of  $\text{TiO}_2$  increases with the concentration of  $\text{TiO}_2$  in bath, and the maximum adding amount is 10gm/l, beyond this value, reaction will be done with the surface of the container. This may be related to components of composite plating solution, dispersion and particle size. J. Novakovic et al.[26], J.N. Balaraju et al.[27] and Komal Yadav et al. [25] have confirmed various factors (such as particle geometry and relative density) affect the adding amount of  $\text{TiO}_2$ . Sina Sadreddini et al.[28] have investigated the influences of different concentrations of  $\text{SiO}_2$  nano particles on deposition rate and corrosion behavior of composite coatings, and found that the deposition rate of nano composite coating was affected by incorporation of  $\text{SiO}_2$  particles.

### *3.3 Influence of the plating time on the deposition rate of the nanoparticle composite plating layer*

Single factor analyses were performed on the orthogonal tests results and the influence of the plating time on the deposition rate of the nanoparticle composite plating layer is shown in Table 3. The plating speed increased at first and then decreased, at longer plating times. The deposition rate of the plating layer was most rapid at a plating time of 1 h. As the plating time increased the plating solution decomposed, and the concentration of active species decreased. The decomposition of the plating solution reduced the deposition rate at longer plating times. Hence, the optimal plating time was determined to be 1 h. CA Leon et al.[29] have studied the effect of plating time on the nickel deposition on silicon carbide particles, and found that uniform nickel films were deposited on the surface of alumina or silicon carbide powders, with a composition ranging from 1.6 to 1.9wt% phosphorus. Aigui Tang et al.[30] have attempted different plating time for Ni–nano- $\text{Al}_2\text{O}_3$ –PTFE coatings and finally determined electroplating time was 2h. Madiha A. Shoeib et al.[31] have adopted the plating time was 1h, its result showed the annealed Ni–P/nano- $\text{TiO}_2$  composite coatings had super corrosion resistance in 3.5% NaCl solution.

### *3.4 Influence of temperature on the deposition rate of nanometer composite plating layer*

Temperature is an important parameter influencing the plating speed of the layer and also influences the stability of the plating solution and the quality of the formed plating layer. Generally, the catalytic reaction for chemical nickel plating only operates with heating above room temperature. When the temperature is high, the plating speed is fast but the stability of the plating solution decreases. We performed single factor analysis on the orthogonal test results, and the influence of

temperature on the deposition rate of the composite plating layer is shown in Table 3. The deposition rate of the plating layer increased when the temperature was increased from 75 to 80°C; however, when the temperature was higher than 80°C, the deposition rate of the plating layer clearly decreased. As temperature increases, the TiO<sub>2</sub> nanoparticles move more rapidly and the catalytic activity of the test specimen surface improves. The deposition rate of the plating layer increases promoting the co-sedimentation of metal ions and TiO<sub>2</sub> particles; however when the temperature increases further, the TiO<sub>2</sub> particles move more energetically and spend less time on the test specimen surface. This effect reduces the co-sedimentation of TiO<sub>2</sub> nanoparticles and nickel. When the temperature is higher than 85°C, air bubbles occur in the plating solution, caused by self-decomposition of the plating solution, and the plating layers that form are loose and of low quality. Thus, the temperature should be maintained at 75–85°C. Temperature is very important to affect the deposition rate in the plating bath. It has been confirmed that useful deposition rates has been achieved at 80–90°C and it has been suggested the bath temperature should be maintained at 85°C[31], the plating bath would become instable above 90°C.

### *3.5 Influence of solution pH on the deposition rate of composite plating layer*

Single factor analyses were performed for the orthogonal test results, and the influence of pH on the deposition rate of the nanometer composite plating layer is shown in Table 3. When the pH value was increased to the range 4–5, the deposition rate of the plating layer increased; however, for pH values higher than 5, the deposition rate of the plating layer decreased. Further increases in solution alkalinity caused the plating solution to become white, caused by Ni<sup>2+</sup> ions changing to Ni(OH)<sub>2</sub>. The plating solution decomposed and the rate of phosphate oxidation to hypophosphite accelerated. The catalytic reaction became a spontaneous reaction and the plating solution was unstable and decomposed. When the pH value was below than 3, the plating speed was slow, and no deposition layer formed on the test specimen. This result was attributed to the difficulty of reducing nickel ions and precipitating nickel at low pH. Considering the deposition rate of the plating layer the solutions should be maintained around pH 5.0. M. Momenzadeh and S. Sanjabi[2] have investigated the effect of pH (3.5, 4.5, 5.5 and 6.5) on the content of TiO<sub>2</sub> and deposition rate, and confirmed high pH resulted in low P content and increased the deposition rate, which is consistent with the results[32]. Madiha A. Shoeib et al.[31] have proposed that the solution pH should be maintained at 4.5 and the deposition rate is very sensitive to the pH values, especially in the acid hypophosphite bath.

### *3.6 Surface morphology of plating surface*

On the basis of the optimized conditions described in sections 3.1 to 3.5, a Ni-P TiO<sub>2</sub> nanoparticle composite plating layer was prepared. The surface morphology and composition of the resulting plating layer are shown in Figures 1 and 2.

The Ni-P plating layer consisted of spherical cells with a mean diameter of 1.5 µm, widely distributed on the surface of the plating layer. As indicated by the energy-dispersive X-ray shown in

Figure 2, these cells contained Ti and O, and the main element contents were as follows Ni (77.87 wt%), P (9.89 wt%), Ti (5.8 wt%) and O (6.44 wt%). These results indicated that the  $\text{TiO}_2$  nanoparticles entered the plating layer and became embedded in the nickel and phosphor alloy; however, Figure 2 also indicated that the distribution of  $\text{TiO}_2$  nanoparticles was uneven in the plating layer, with some slight agglomeration. S.A. Abdel. Gawad et al.[33] and Zhou, Y. et al.[34] showed the same results. Madiha A. Shoeib et al.[31] have found the morphology of Ni-P- $\text{TiO}_2$  exhibited a coarse nodular compact structure, which was revealed the presence of  $\text{TiO}_2$  particles apart from nickel and phosphorus on nodules, and found the Ti and O content in the coating increased with the  $\text{TiO}_2$  nanoparticles increasing from 1 g/l to 5 g/l.

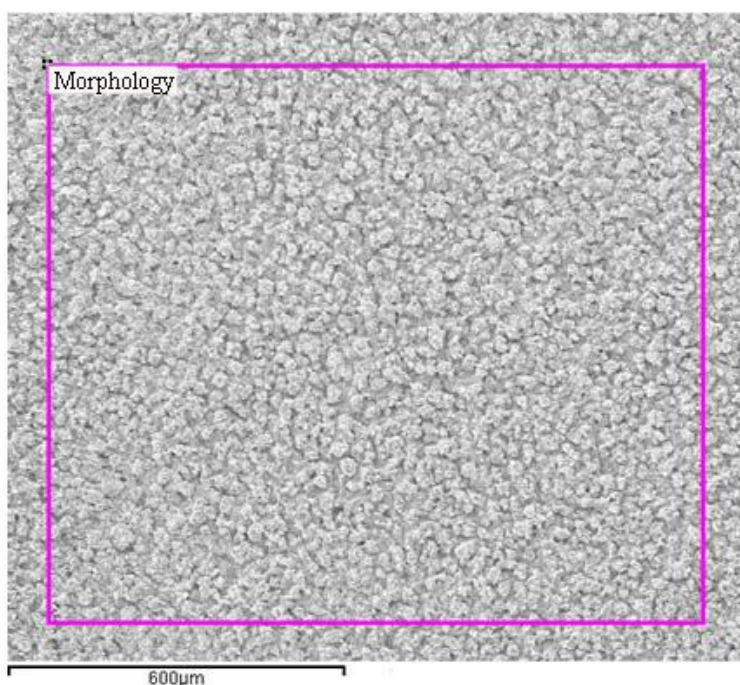


**Figure 1.** Morphology of Ni-P  $\text{TiO}_2$  nanoparticle composite plating layer

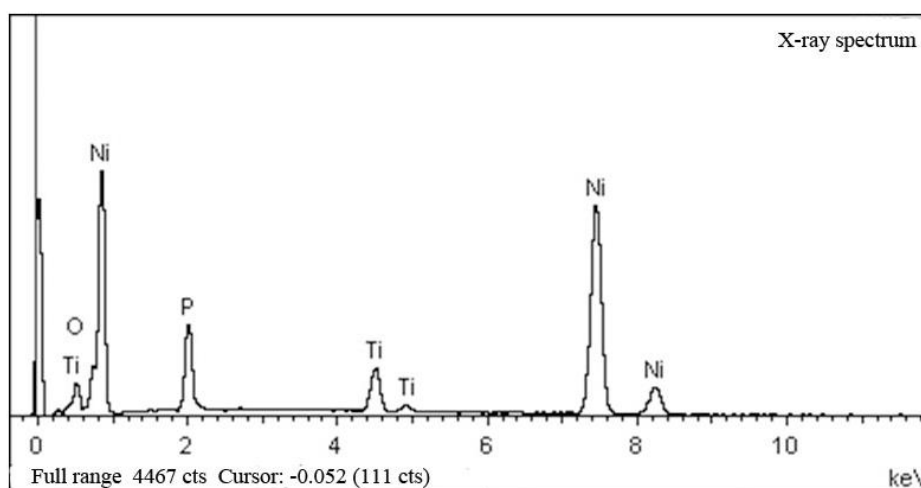


**Figure 2.** Energy-dispersive X-ray spectrum of Ni-P nanometer  $\text{TiO}_2$  chemical composite plating layer



### 3.7 Polarization measurements of plating layer

Figure 3 shows the Tafel polarization curves of the carbon steel matrix, the Ni-P plating layer, and the Ni-P TiO<sub>2</sub> nanoparticle composite plating layer in the 3.5% NaCl solution. The corrosion potentials, corrosion current density, anodic tafel slopes and cathodic tafel slopes of the matrix carbon steel were  $\phi_c = -0.505$  V,  $i_{corr} = 1.57 \times 10^{-4}$  A/cm<sup>2</sup>,  $b_a = 0.0592$  V/dec and  $b_c = 0.0775$  V/dec, respectively. The corrosion potentials, corrosion current density, anodic tafel slopes and cathodic tafel slopes of the Ni-P plating layer were  $\phi_c = -0.351$  V,  $i_{corr} = 1.08 \times 10^{-5}$  A/cm<sup>2</sup>,  $b_a = 0.0362$  V/dec, and  $b_c = 0.0224$  V/dec. The corrosion potentials, corrosion current density, anodic tafel slopes and cathodic tafel slopes of the Ni-P TiO<sub>2</sub> plating layer were  $\phi_c = -0.381$  V,  $i_{corr} = 7.11 \times 10^{-6}$  A/cm<sup>2</sup>,  $b_a = 0.0305$  V/dec and  $b_c = 0.0208$  V/dec. The Ni-P TiO<sub>2</sub> nanoparticle composite plating layer and the Ni-P plating layer exhibited a lower corrosion currents density than the carbon steel matrix, and the corrosion current density of Ni-P TiO<sub>2</sub> nanoparticle composite plating layer was lower than that of the Ni-P plating layer. These results indicate that, after the TiO<sub>2</sub> nanoparticles were added to the Ni-P plating layer, the corrosion resistance of the Ni-P TiO<sub>2</sub> nanoparticle composite plating layer was improved compared with that of the Ni-P plating layer, and both layers showed higher corrosion resistance than that of the carbon steel matrix. Cheng-Kuo Lee[16] had ever reported the similar result. There were also no passivation tendency to be observed in the tese range, this was consistent with the result of M. Momenzadeh and S. Sanjabi[2]. J. Novakovic et al.[26, 35] and M. Momenzadeh et al.[2] had verified that, as the TiO<sub>2</sub> nanoparticles were added to the Ni-P plating layer, the co-deposition of particles and Ni-P alloy would speed up the passivation process of the nickel, which can increase the corrosion resistance of the composite plating layer.

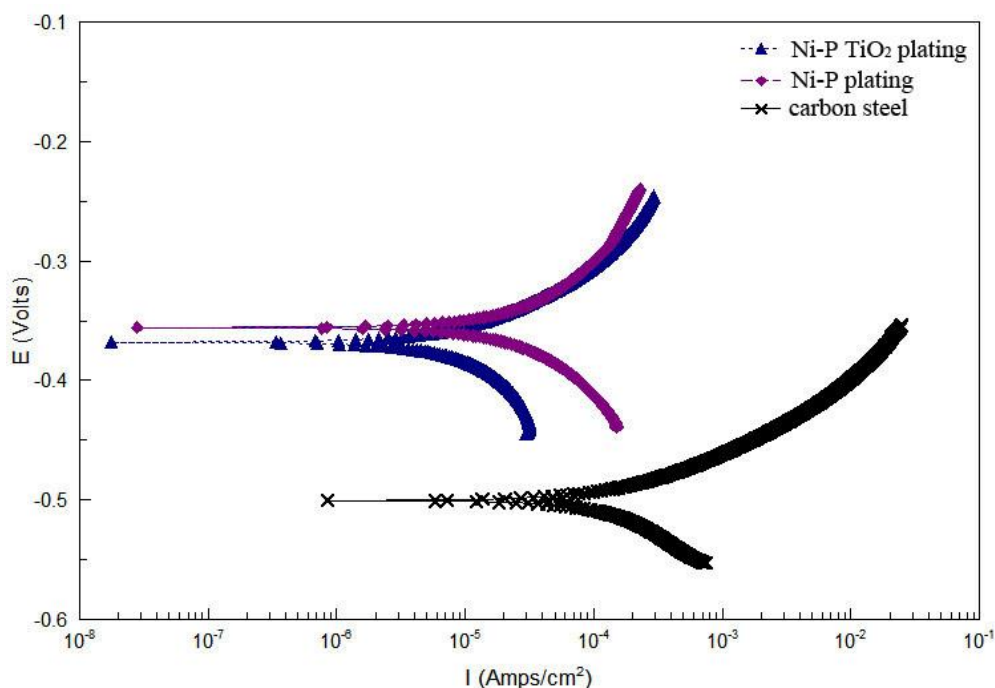


**Figure 3.** Polarization curves of Ni-P TiO<sub>2</sub> nanoparticle composite plating layer, Ni-P plating layer and carbon steel matrix in 3.5% NaCl

### 3.8 Immersion corrosion tests of plating layers

The specimens were placed in standard corrosion solutions of 10%  $\text{H}_2\text{SO}_4$  and 15%  $\text{HCl}$ , and after 9 h at room temperature, the mean corrosion rates were calculated from the mass difference of the test specimens before and after the corrosion. The , Ni-P  $\text{TiO}_2$  nanoparticle composite and Ni-P plating layer specimens showed weight losses of 0.450, 0.032, and 0.027  $\text{g}/\text{cm}^2$ , respectively. The carbon steel matrix had the lowest corrosion resistance, while those of the Ni-P  $\text{TiO}_2$  nanoparticle composite plating layer and the Ni-P plating layer were similar. The corrosion resistance of the Ni-P plating layer was slightly better than that of the Ni-P  $\text{TiO}_2$  nanoparticle composite plating layer.

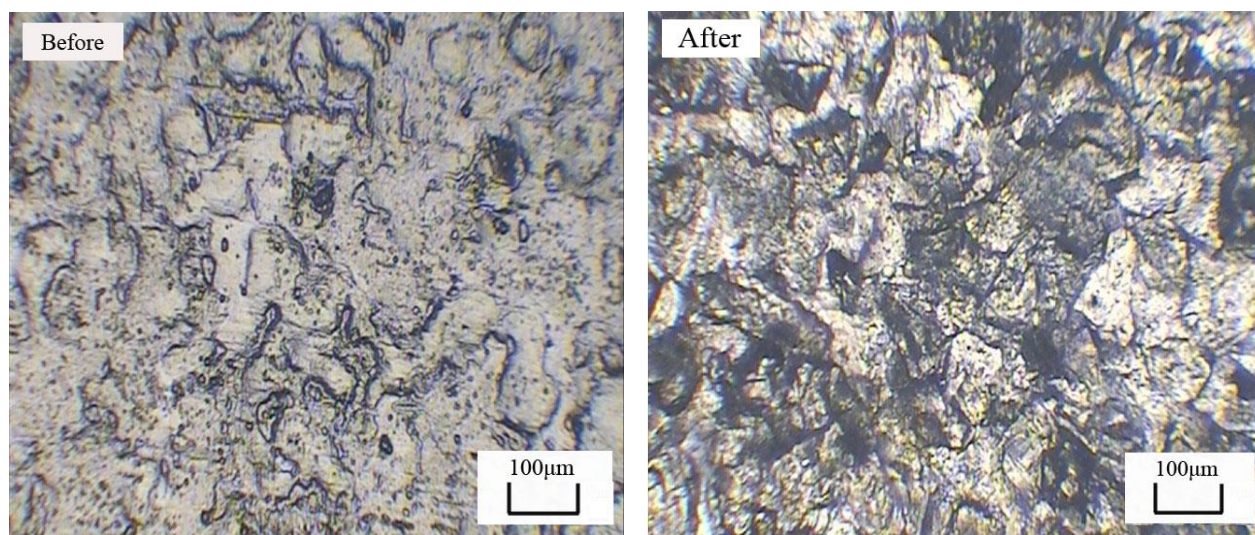


**Figure 4.** Surface morphologies of carbon steel matrix before and after corrosion testing in standard corrosion solutions of 10%  $\text{H}_2\text{SO}_4$  and 15%  $\text{HCl}$

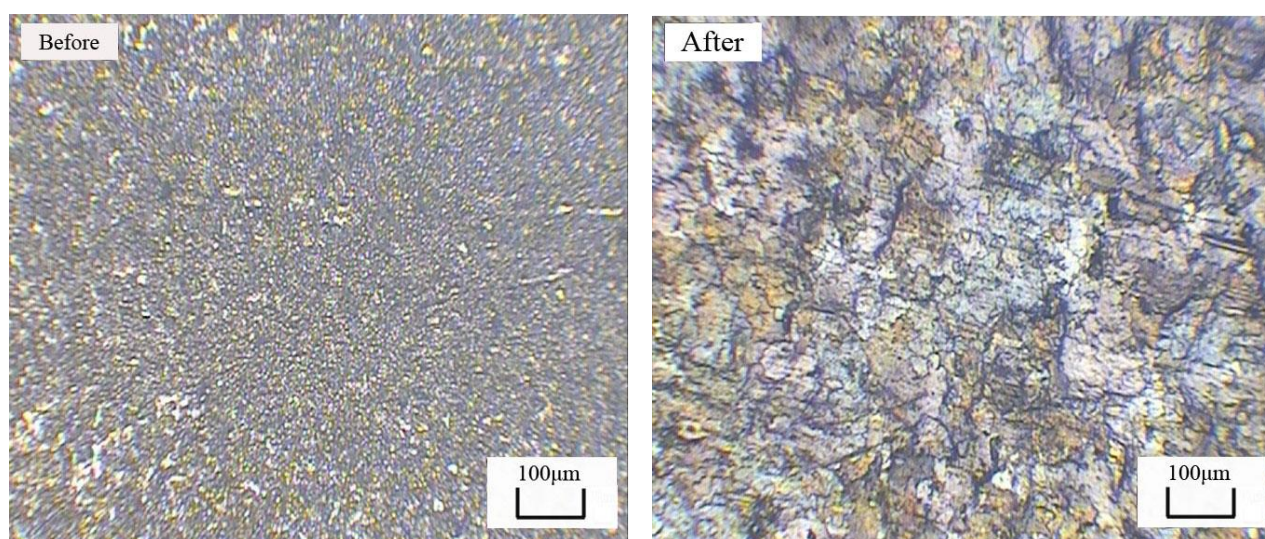


**Figure 5.** Surface morphologies of Ni-P plating layer before and after corrosion testing in standard corrosion solutions of 10%  $\text{H}_2\text{SO}_4$  and 15%  $\text{HCl}$



Figures 4 to 6 show the surface morphologies of the test specimens before and after corrosion testing. The test specimen of the carbon steel matrix was severely corroded, and featured many concave-surface pits on its surface. Conversely the surface of the Ni-P plating layer was slightly corroded with a flat appearance; and the surface of the Ni-P TiO<sub>2</sub> nanoparticle composite layer featured slightly higher corrosion than that of the Ni-P plating layer, with a few pits appearing on its surface. Thus, the Ni-P TiO<sub>2</sub> nanoparticle composite plating layer had similar corrosion resistance to that of the Ni-P plating layer. Both layers had clearly better corrosion resistance than that of the carbon steel matrix. Madiha A. Shoeib et al.[31] have investigated the corrosion resistance of Ni-P/nano-TiO<sub>2</sub> coatings in 3.5% NaCl solution by Tafel plots and electrochemical impedance spectroscopic, and found the as-plated composite coating had superior corrosion resistance over Ni-P coating.

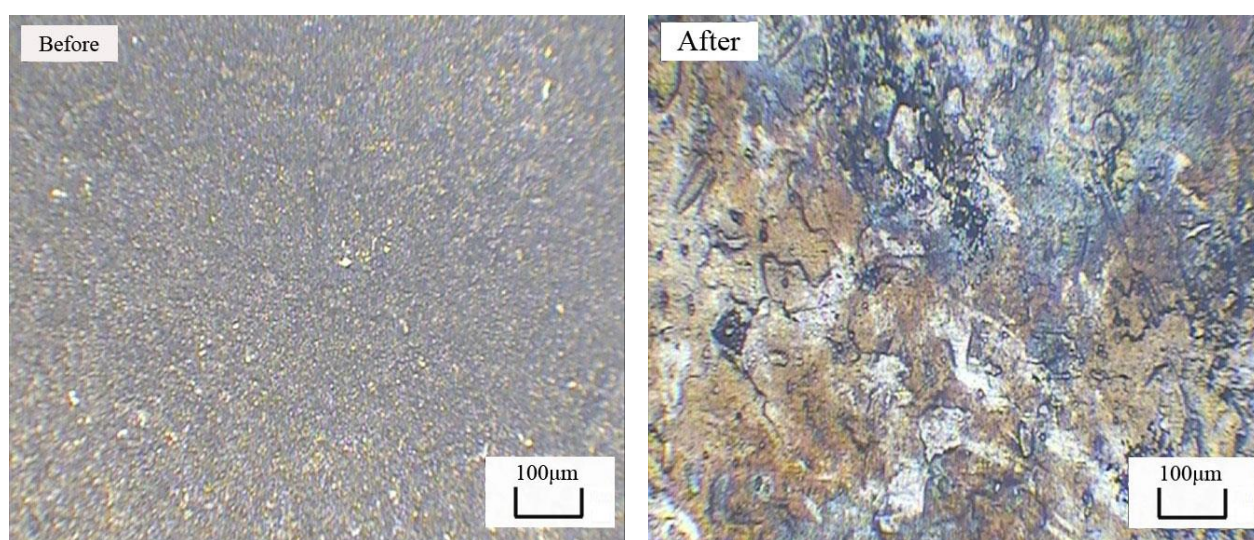


**Figure 6.** Surface morphologies of Ni-P TiO<sub>2</sub> nanoparticle composite plating layer before and after corrosion testing in standard corrosion solutions of 10% H<sub>2</sub>SO<sub>4</sub> and 15% HCl

The Ni-P TiO<sub>2</sub> composite plating layer was obtained by embedding TiO<sub>2</sub> nanoparticles in the non-crystalline Ni-P plating layer, while retaining the advantageous properties of the Ni-P plating layer. In non-crystal structures, crystal defects such as grain boundaries, dislocations and segregation that are present in crystal alloys are eliminated, leading to the high corrosion resistance of the Ni-P TiO<sub>2</sub> composite plating layer. All the plating layers prepared in these tests had P contents of about 10%, and featured high-phosphor alloy plating layers. As the P content increased, the formation rate of the plating layer increased, and the plating became more dense. However, the plating layer became uneven when TiO<sub>2</sub> nanoparticles were added. The surface features also have different electrode potentials in the corrosion medium. Thus, many micro-electrodes are generated, which act as micro-corrosion sites. The porosity and surface roughness of the plating layer increased when the TiO<sub>2</sub> nanoparticles were added; thus, the corrosion resistance of the Ni-P TiO<sub>2</sub> nanoparticle composite plating layer was lowered, and its corrosion resistance was slightly lower than that of the Ni-P plating layer.

#### 4. CONCLUSION

1. In a Ni-P TiO<sub>2</sub> nanoparticle composite plating process, the rate of deposition tended to first increase and then decrease with increasing plating time. The optimum time for the plating was about 1 h. The temperature should be maintained at 75–85 °C. The deposition rate of the plating layer was highest when the TiO<sub>2</sub> nanoparticle content was 3 g/L. The deposition rate was highest in a solution pH of 5.0.

2. Polarization measurements and immersion tests were used to compare the corrosion resistance of different plating layers. The corrosion resistance of the Ni-P TiO<sub>2</sub> nanoparticle composite plating layer was higher than that of the Ni-P alloy plating layer without TiO<sub>2</sub> nanoparticles in the 3.5% NaCl solution. The corrosion resistance of the Ni-P plating layer was slightly better than that of the Ni-P TiO<sub>2</sub> nanoparticle composite plating layer which immersed in the 10% H<sub>2</sub>SO<sub>4</sub> and 15% HCl solution. However, both these layers featured higher corrosion resistance than that of the carbon steel matrix.

#### ACKNOWLEDGMENTS

The authors gratefully acknowledge the financial supports from the Key Scientific Research Projects of Higher Education of Henan Province of China (No. 14A430010), Science and Technology Project Foundation of Xinxiang City (No. ZG15010) and Key Teacher and Bainong Talent Foundation of Henan Institute of Science and Technology.

#### References

1. I. Ohno, *Mater. Sci Eng. A*, 146 (1991) 33.
2. M. Momenzadeh and S. Sanjabi, *Mater. Corros.*, 63 (2012) 614.
3. J.-G. Jin, S.-K. Lee, and Y.-H. Kim, *Thin Solid Films*, 466 (2004) 272.
4. Q. Yang, S. Liang, J. Wang, and Y. Wang, *Sci. China Technol. Sci.*, 56 (2013) 1147.
5. W. Chen, W. Gao, and Y. He, *J. Sol-Gel Sci. Techn.*, 55 (2010) 187.
6. J. Hosseini and A. Bodaghi, *Surf. Eng.*, 29 (2013) 183.
7. J. Calderón, J. Jiménez, and A. Zuleta, *Surf. Coat. Technol.*, 304 (2016) 167.
8. T. Radu, M. Vlad, F. POTECASU, and G. Istrate, *Dig. J. Nanomater Bios.*, 10 (2015) 1055.
9. Y. Wang, W. Chen, A. Shakoor, R. Kahraman, W. Lu, B. Yan, and W. Gao, *Int. J. Electrochem. Sci.*, 9 (2014) 4384.
10. W. Chen, W. Gao, and Y. He, *Surf. Coat. Technol.*, 204 (2010) 2493.
11. P. Gadhari and P. Sahoo, *Surf. Rev. Lett.*, 23 (2016) 1550082.
12. V. Niksefat and M. Ghorbani, *J. Alloys Compd.*, 633 (2015) 127.
13. H.-L. Wang, L.-Y. Liu, Y. Dou, W.-Z. Zhang, and W.-F. Jiang, *Appl. Surf. Sci.*, 286 (2013) 319.
14. A. Farzaneh, M. Mohammadi, M. Ehteshamzadeh, and F. Mohammadi, *Appl. Surf. Sci.*, 276 (2013) 697.
15. P. Gadhari and P. Sahoo, *Int. J. Surf. Eng. Interdiscipl Mater. Sci.*, 3 (2015) 18.
16. C.-K. Lee, *Int. J. Electrochem. Sci.*, 7 (2012) 12941.
17. M. Sarret, C. Müller, and A. Amell, *Surf. Coat. Technol.*, 201 (2006) 389.
18. Y. Yang, W. Chen, C. Zhou, H. Xu, and W. Gao, *Appl. Nanosci.*, 1 (2011) 19.
19. L. Yan, S.-r. Yu, J.-D. Liu, Z.-W. Han, and D.-s. Yuan, *Trans. Nonferrous Met. Soc. China*, 21 (2011) 483.

20. M. Hosseini, M. Abdolmaleki, S. Ashrafpoor, and R. Najjar, *Surf. Coat. Technol.*, 206 (2012) 4546.
21. M. Mohammadi and M. Ghorbani, *J. Coat. Technol. Res.*, 8 (2011) 527.
22. J. Balaraju and K. Rajam, *Surf. Coat. Technol.*, 200 (2006) 3933.
23. X. W. Guo, S. H. Wang, H. Y. Yang, L. M. Peng, and W. J. Ding, *Mater. Sci. Forum*, 690 (2011) 422.
24. L. Z. Song, S. Z. Song, and J. Zhao, *Acta Metall. Sin.*, 19 (2006) 117.
25. V. U. Komal Yadav, R. K. Duchaniya, *J. Mater. Sci. Surf. Eng.*, 4 (2016) 410.
26. J. Novakovic, P. Vassiliou, K. Samara, and T. Argyropoulos, *Surf. Coat. Technol.*, 201 (2006) 895.
27. J. N. Balaraju, T. S. N. S. Narayanan, and S. K. Seshadri, *J. Appl Electrochem*, 33 (2003) 807.
28. S. Sadreddini and A. Afshar, *Appl. Surf. Sci.*, 303 (2014) 125.
29. C. A. Leon and R. A. L. Drew, *J. Mater. Sci.*, 35 (2000) 4763.
30. A. Tang, M. Wang, W. Huang, and X. Wang, *Surf. Coat. Technol.*, 282 (2015) 121.
31. M. A. Shoeib, M. M. Kamel, S. M. Rashwan, and O. M. Hafez, *Surf. Interface Anal.*, 47 (2015) 672.
32. A. A. Aal, Z. I. Zaki, and Z. A. Hamid, *Mater. Sci. Eng. A*, 447 (2007) 87.
33. S. A. A. Gawad, A. M. Baraka, M. S. Morsi, and M. S. A. Eltoum, *Int. J. Electrochem. Sci.*, 8 (2013) 1722.
34. Y. Zhou, H. Zhang, and B. Qian, *Appl. Surf. Sci.*, 253 (2007) 8335.
35. J. Novakovic and P. Vassiliou, *Electrochim. Acta*, 54 (2009) 2499.